Papers submitted to the Conference "Applications of Physics in Mechanical and Material Engineering"

Simulation of The Impact of Bulk Selenium Composition Variation in CIGSSe Solar Cell

G.M. Albalawneh[a,*], M.M. Ramli[b,d], M.Z.M. Zain[c], Z. Sauli[b,d], M. Nabiałek[e] and K. Jeż[e]

[a] *Institute of Nano Electronic Engineering, Universiti Malaysia Perlis, 01000 Kangar, Perlis, Malaysia*
[b] *Faculty of Electronic Engineering Technology, Universiti Malaysia Perlis (UniMAP), Pauh Putra Campus, 02600, Arau, Perlis, Malaysia*
[c] *Faculty of Mechanical Engineering Technology, Universiti Malaysia Perlis (UniMAP), Pauh Putra Campus, 02600, Arau, Perlis, Malaysia*
[d] *Geopolymer and Green Technology (CeGeoGTech), Universiti Malaysia Perlis (UniMAP), Pauh Putra Campus, 02600, Arau, Perlis, Malaysia*
[e] *Department of Physics, Faculty of Production Engineering and Materials Technology, Czestochowa University of Technology, al. Armii Krajowej 19, 42-200 Częstochowa, Poland*

Doi: 10.12693/APhysPolA.142.28 *e-mail: mmahyiddin@unimap.edu.my

This study analytically investigates the effect of different ratios of elemental sulphur to elemental selenium on the performance of chalcopyrite Cu(In,Ga)(S,Se)$_2$ (CIGSSe) thin-film solar cell. The influence of the various ratios $x = S/(S + Se)$ on photovoltaic parameters was simulated using Solar Cell Capacitance Simulator software. The simulated band diagram for both Cu(In,Ga)S$_2$ (CIGS) and Cu(In,Ga)Se$_2$ (CIGSe) shows band banding at the back of the CIGS layer, whereas in CIGSe it is flat; this brings to the fore the issue of back contact in high content sulphur absorbers. The simulation for quantum efficiency shows that the band edge of the solar cell device is shifted to a shorter wavelength with increasing sulphur content. Generally, Se incorporation improves photovoltaic parameters and consequently enhances the solar cell performance. The optimal stoichiometry was obtained for CuIn$_{0.7}$Ga$_{0.3}$(S$_{0.3}$Se$_{0.7}$)$_2$, CIGSe, and CIGS with an efficiency of 18.4%, 17.5%, and 11.3%, respectively.

topics: CIGS solar cells, sulfurization, thin films, selenization

1. Introduction

Thin-film solar cells such as CIGSe based devices have attracted more attention over the last decade as a potential alternative for the costly silicon-based photovoltaic (PV), widely used in solar cell production [1, 2]. Given the development that has been made to progress the CIGSe conversion efficiency, it is found that the CIGSe absorber bandgap can be controlled either by Ga or S alloying [3, 4]. The beneficial effects of S alloying are extensively reported in Cu(In,Ga)(Se,S)$_2$ solar cells, especially in the case of the S-rich surface of the CIGSe absorber layer [5–7]. However, very limited works reported on the numerical or theoretical effects of the $x = S/(S + Se)$ ratios. Up to now, the most reported papers focused on optimising the S-enriched surface of CIGSSe abserbers. In contrast, few works have reported the effect of S-alloying onto the absorber bulk.

In this work, 1D Solar Cell Capacitance Simulator (SCAPS) tool was used to simulate photovoltaic parameters in different x ratios for the CuInGa(S$_x$Se$_{1-x}$)$_2$ absorbers.

2. Methodology

In the present work, numerical modelling of CIGSSe thin-film solar cells was carried out using Solar Cell Capacitance Simulator software (SCAPS. 1D version 3.3.02). The fundamental cell configuration used consisted of Mo/CIGSe/CdS/i:ZnO/ZnO:Al. The bandgap of the absorber layer varies in the range of 1.18–1.76 eV due to the variation of the selenium ratio in the layer. The thickness of the absorber layer varied in the range of 0.5–2.5 μm.

The parameters for the simulated device are extracted from reliable numerical models and experimental studies [8–10]. The simulation was

TABLE I

The variations of stoichiometry and band gap with the doping factor x for $CuIn_{0.7}Ga_{0.3}(S_xSe_{1-x})_2$.

Doping factor	Stoichiometry	Bandgap [eV]
$x = 0.0$	$CuIn_{0.7}Ga_{0.3}Se_2$	1.17670
$x = 0.1$	$CuIn_{0.7}Ga_{0.3}(S_{0.2}Se_{1.8})$	1.23532
$x = 0.2$	$CuIn_{0.7}Ga_{0.3}(S_{0.4}Se_{1.6})$	1.29394
$x = 0.3$	$CuIn_{0.7}Ga_{0.3}(S_{0.6}Se_{1.4})$	1.35256
$x = 0.4$	$CuIn_{0.7}Ga_{0.3}(S_{0.8}Se_{1.2})$	1.41118
$x = 0.5$	$CuIn_{0.7}Ga_{0.3}(S_1Se_1)$	1.46980
$x = 0.6$	$CuIn_{0.7}Ga_{0.3}(S_{1.2}Se_{0.8})$	1.52842
$x = 0.7$	$CuIn_{0.7}Ga_{0.3}(S_{1.4}Se_{0.6})$	1.58704
$x = 0.8$	$CuIn_{0.7}Ga_{0.3}(S_{1.6}Se_{0.4})$	1.64566
$x = 0.9$	$CuIn_{0.7}Ga_{0.3}(S_{1.8}Se_{0.2})$	1.70428
$x = 1.0$	$CuIn_{0.7}Ga_{0.3}S_2$	1.76290

performed on the basis of the composition variation to study the effect of sulphur content on solar cell performance, i.e., η, V_{oc}, J_{sc}, FF. After optimising the sulphur content, the CIGSSe solar cell thickness was reduced to 0.5 μm to test the performance of the ultra-thin device with optimum sulphur content.

3. Results and discussion

Several reports on the bandgap variation as a function of the Ga/In or S/Se compositions in binary, ternary and quaternary Cu-based chalcopyrite compounds can be found [11–13]. In [14], an expression was introduced to evaluate the bandgap energy (E_g) for the pentanary $Cu(In_{1-y},Ga_y)(S_xSe_{1-x})_2$ compound. Its form is given as

$$E_g^{(\mathrm{CIGSSe})}(y,x) = (1-x)\left[(1-y)\,E_g{}^{(\mathrm{CISSe})}(x) + y\,E_g{}^{(\mathrm{CGSSe})}(x) - b^{(\mathrm{CIGSe})}y(1-y)\right]$$
$$+x\left[(1-y)\,E_g^{(\mathrm{CISSe})}(x) + y\,E_g{}^{(\mathrm{CGSSe})}(x) - b^{(\mathrm{CIGS})}\,y(1-y)\right], \quad (1)$$

where b is the optical bowing coefficients, and y and x are $\mathrm{Ga}/(\mathrm{Ga}+\mathrm{In})$ and $\mathrm{S}/(\mathrm{Se}+\mathrm{S})$, respectively. In the case of the Ga ratio, it was proved that the $y = 0.3$ ratio is optimal to achieve the highest photovoltaic efficiency [15]. Thus, in this work, the targeted stoichiometry of the absorber was $Cu_{0.92}In_{0.7}Ga_{0.3}(S,Se)_2$, i.e., with $y = 0.3$. After applying the bandgap and consistent optical bowing constants for the compounds [16], the evaluated bandgap values from (1) for different S values are calculated and listed in Table I.

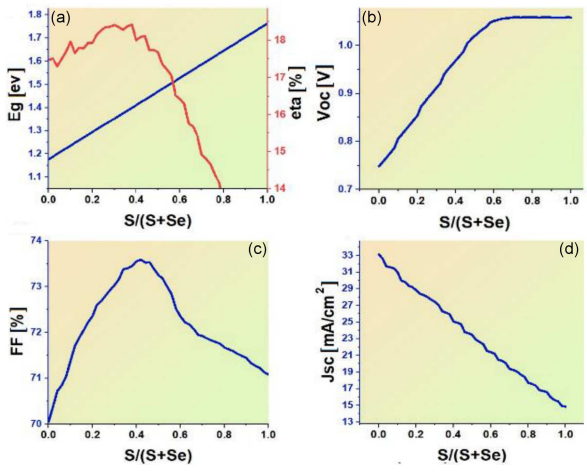

Fig. 1. (a) Variation of the bandgap E_g [eV] (blue line) and efficiency (red line) with different ratios of S/(S+Se). Variation of (b) open circuit voltage V_{oc}, (c) short circuit current J_{sc}, and (d) fill factor FF variation with different S/(S+Se) ratios.

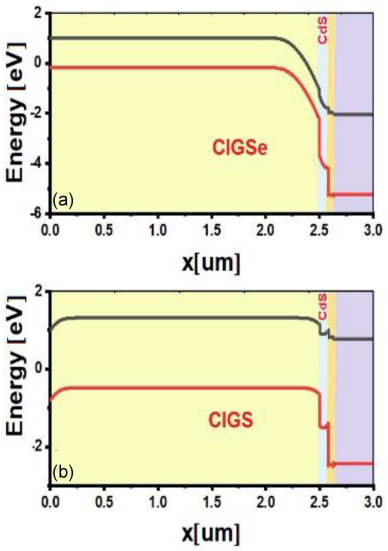

Fig. 2. Simulated energy band diagrams of (a) CIGSe (b) CIGS solar cells.

Figure 1a–d shows the simulated CIGSSe parameters V_{oc}, J_{sc}, FF, as well as the conversion efficiency as a function of sulphur content $x = \mathrm{S}/(\mathrm{S}+\mathrm{Se})$. The efficiency simulation results are shown in Fig. 1a. The maximum efficiency achieved for the ratio $x \simeq 0.3$ corresponds to the bandgap of about 1.35 eV, which is in good agreement with the value reported in [17]. In the case of J_{sc}, Fig. 1d shows an almost linear decrease of J_{sc} in the range under investigation. The observed trend

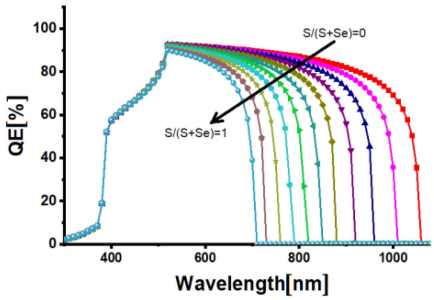

Fig. 3. Quantum efficiency QE for a number of selenium composition ratios.

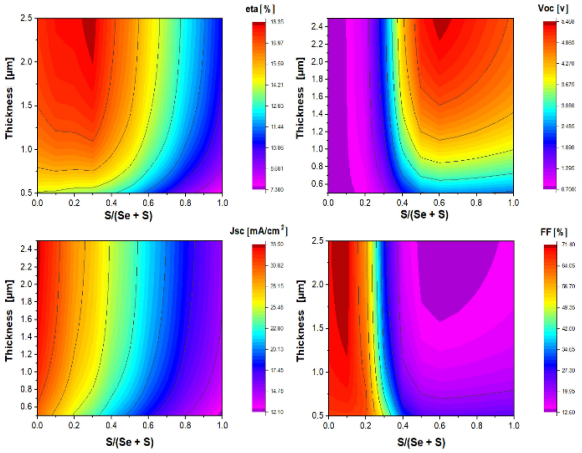

Fig. 4. Combined effect of changing the composition parameter x and the absorber layer thickness on (a) efficiency, (b) short circuit current, (c) open circuit voltage V_{oc} (d) fill factor FF.

is explained by a decrease in photon absorption due to the overall increase of the bandgap. Figure 1b depicts the variation of V_{oc}, an increase in the range from 744 to 1057 mV shows an increasing trend with increasing S content. However, when $x > 0.6$, the behaviour of V_{oc} exhibits no change due to the large conduction band offset. On the other hand, for the same reason, a reduced FF value is obtained for J_{sc} as shown in Fig. 1c.

To further understand the performance of photovoltaic, the energy band structure is essential. Figure 2 illustrates simulated schematic diagrams of the band alignment on the heterojunction interface between (a) n-CdS/p-CIGSe and (b) n-CdS/p-CIGS. In the back contact interface, the banding is present only in pure sulphide CIGS. This rear banding can be explained by the large bandgap which commonly leads to limited back contact performance.

Simulated quantum efficiency (QE) spectrum with different selenium compositions under the AM1.5 G solar spectrum are shown in Fig. 3. The shift of QE towards lower wavelengths (higher energies) with increasing S content was expected due to the increased bandgap.

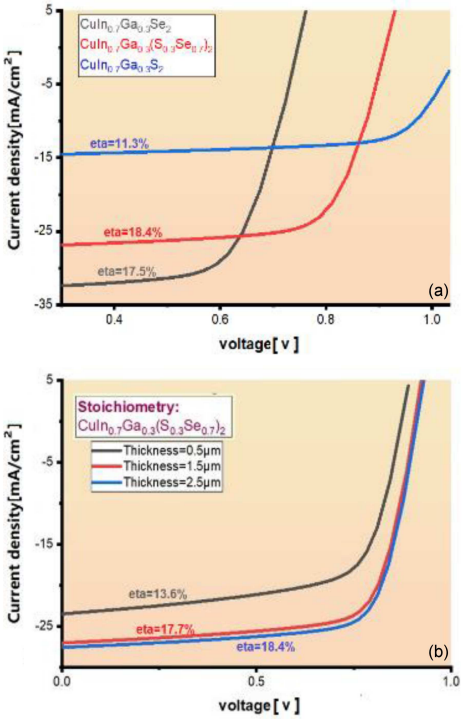

Fig. 5. (a) The comparative J–V curve of the solar cell based on 3 difference stoichiometry absorbers of different S content $x = 0, 0.3$ and $x = 1$. (b) The efficiency as a function of the absorber thickness (0.5, 1.5, 2.5 μm) for based solar cells.

The combined simultaneous influence of absorber thickness with various S/(S+Se) absorber content on the performance of the CIGSSe solar cell is shown in Fig. 4. The contour area of the highest J_{sc} values extends in the region with the highest thickness and maximum selenium content of the absorption layer (see Fig. 4a). Meanwhile, for a higher sulphur content $x > 0.4$, increasing the absorber layer thickness causes the systematic effect of increasing V_{oc}. For thicker absorbers, a higher sulphur content in the range of $x = 0.5$–0.7 results in a significant increase in the value of V_{oc}. At lower selenium content $x < 0.4$, FF increases with the absorber layer thickness, the height contour area of FF is found at the relatively lower sulphur content, and high absorber thickness, low FF values appear at the higher x and thicker absorbers. Therefore, higher S/(S+Se) concentrations caused a steep drop-off in the efficiency due to the decreased FF.

The final J–V curve plots for the simulated in the case of pure selenide ($x = 0$), pure sulfide ($x = 1$), and mixed selenide sulfide with ($x = 0.3$) are shown in Fig. 5a. Moreover, the efficiency of the absorbers with optimum stoichiometry as a function of their thickness is shown in Fig. 5b. The efficiency of 13.6% for an ultra-thin absorber layer of 0.5 μm thickness was of about 26% less than the efficiency of the same device of 2.5 μm thickness absorber.

4. Conclusions

This work investigates the effect of different S ratios ($x = S/(S+Se)$) on the photovoltaic performance of the $CuIn_{0.7}Ga_{0.3}(S_XSe_{1-X})_2$ solar cells. The maximum conversion efficiency is obtained with the stoichiometry of $CuIn_{0.7}Ga_{0.3}(S_{0.3}Se_{0.7})_2$ corresponding to the bandgap 1.35 eV. The comparative band diagram of the fully sulphide CIGS and fully selenide CIGSe highlights the noticeable rear band banding and unsatisfactory back-contact in CIGSe. The cut-off wavelength in QE has shifted towards the shorter wavelengths with increasing Se. In simulations, we observed that parameters like the flat back band banding and the optimal band gap provide higher QE in selenium substitute compositions. Therefore, the performance of selenium, substituted for $x < 0.7$, is superior than that of pure CIGS. Overall comparative J–V plot shows the efficiency of 18.4% for $CuIn_{0.7}Ga_{0.3}(S_{0.3}Se_{0.7})_2$, 17.7% for CIGSe and 11.3% for CIGS solar cell.

References

[1] T.D. Lee, A.U. Ebong, *Renew. Sustain. Energy Rev.* **70**, 1286 (2017).

[2] M.A. Green, *J. Mater. Sci. Mater. Electron.* **18**, 15 (2007).

[3] S. Béchu, A. Loubat, M. Bouttemy, J. Vigneron, J.L. Gentner, A. Etcheberry, *Thin Solid Films.* **669**, 425 (2019).

[4] M. Saifullah, J.H. Moon, S.J. Ahn, J. Gwak, S. Ahn, K. Kim, Y.J. Eo, J.H. Yun, *Curr. Appl. Phys.* **16**, 1517 (2016).

[5] Y. Xie, H. Chen, A. Li, X. Zhu, L. Zhang, M. Qin, Y. Wang, Y. Liu, F Huang, *J. Mater. Chem. A.* **2**, 13237 (2014).

[6] S.H. Lin, J.C. Sung, C.H. Lu, *Thin Solid Films* **616**, 746 (2016).

[7] Y.I. Kim, K.J. Yang, S.Y. Kim, J.K. Kang, J. Kim, W. Jo, H. Yoo, J.H. Kim, D.H. Kim, *J. Ind. Eng. Chem.* **76**, 437 (2019).

[8] T. Zhang, Y. Yang, D. Liu, S.C. Tse, W. Cao, Z. Feng, S. Chen, L. Qian, *Energy Environ. Sci.* **9**, 3674 (2016).

[9] E.M.K.I. Ahamed, M.A. Matin, N. Amin, in: *4th Int. Conf. on Advances in Electrical Engineering (ICAEE), Dhaka 2017*, IEEE, 2017, p. 681.

[10] T. Minemoto, T. Matsui, H. Takakura, Y. Hamakawa, T. Negami, Y. Hashimoto, T. Uenoyama, M. Kitagawa, *Sol. Energy Mater. Sol. Cells* **67**, 83 (2001).

[11] J.H. Boyle, B.E. McCandless, W.N. Shafarman, R.W. Birkmire, *J. Appl. Phys.* **115**, (2014).

[12] M. Turcu, I.M. Kötschau, U. Rau, *J. Appl. Phys.* **91**, 1391 (2002).

[13] S.H. Wei, A. Zunger, *J. Appl. Phys.* **78**, 3846 (1995).

[14] M. Bär, W. Bohne, J. Röhrich, E. Strub, S. Lindner, M.C. Lux-Steiner, C.H. Fischer, T.P. Niesen, F. Karg, *J. Appl. Phys.* **96**, 3857 (2004).

[15] S.H. Song, K. Nagaich, E.S. Aydil, R. Feist, R. Haley, S.A. Campbell, in: *35th IEEE Photovoltaic Specialists Conf., Honolulu (HI) 2010*, IEEE, 2010, p. 2488.